Optical Anisotropy of Oxidized Si(001) Surfaces and Its Oscillation in the Layer-By-Layer Oxidation Process

T. Yasuda* and S. Yamasaki

Joint Research Center for Atom Technology (JRCAT), National Institute for Advanced Interdisciplinary Research (NAIR), 1-1-4 Higashi, Tsukuba 305-8562, Japan

M. Nishizawa, N. Miyata, A. Shklyaev, and M. Ichikawa

Joint Research Center for Atom Technology (JRCAT), Angstrom Technology Partnership (ATP), 1-1-4 Higashi, Tsukuba 305-0046, Japan

T. Matsudo and T. Ohta

Tokyo Electron Limited, Technology Development Center, 650 Mitsuzawa Hosaka-cho, Nirasaki 407-0192, Japan

Reflectance-difference (RD) measurements for the oxidation of single-domain (2×1)-reconstructed Si(001) surfaces show that the polarity of the interface-induced optical anisotropy is reversed repeatedly with increasing oxide thickness. The oscillation of the RD amplitude, which we show is due to layer-by-layer progression of the oxidation, has allowed us to count the number of oxidized Si layers *in situ* during oxidation. The origins of the observed spectral line shape are discussed.

PACS numbers: 78.68.+m, 81.65.Mq

The study of the oxidation of Si has a long history [1]. Since insulating SiO_2 layers and SiO_2-Si interfaces are important for semiconductor technology, extensive efforts have been made to understand the oxidation phenomena. The continuing downscaling of metal-oxide-semiconductor devices now requires gate insulators thinner than 2 nm, prompting research on the initial stages of the oxidation process [2]. Recent experiments using transmission electron microscopy [3] and scanning reflection electron microscopy [4] have unambiguously shown that the oxidation of Si proceeds in the layer-by-layer mode on both the (001) and (111) faces. On the (2×1)-reconstructed (001) surface, there exist two kinds of domains with twofold symmetry, which differ in the direction of their dimer bonds, $[\bar{1}10]$ and $[110]$. When this surface is oxidized in the layer-by-layer mode, completion of the oxidation of every monolayer is associated with a rotation of the symmetry axis of each domain by 90°. If this switching of the symmetry axis is detectable in real time by some means, one can measure the oxidation rate for each monolayer. Combination of such layer-resolved kinetic experiments with the first-principles calculations [5] shall advance our understanding of the physical and chemical mechanisms of the oxidation process.

One of the potential techniques for such observation is reflectance-difference (or reflectance-anisotropy) spectroscopy (RDS or RAS) which measures the difference between the normal-incidence reflectances of light polarized along two orthogonal axes [6,7]. The two types of the domains on the Si(001) face generate RD signals of opposite polarities. The necessary condition for us to observe a nonzero net RD signal on the (001) face is to prepare such a surface that is dominated by one of the domains in the coverage, which we call a single-domain surface. The RD spectra for single-domain 2×1 surfaces prepared by utilizing the electromigration effect [8] and an intentional miscut of the crystal [9] have been reported in the literature [10–12].

In this Letter, we examine the changes in the RD spectra as the single-domain Si(001) surface is oxidized in the layer-by-layer mode. We will show that the switching of the symmetry axis is indeed observed as an oscillation of the RD signal. The obtained RD spectra exhibit spectral line shapes of the energy-derivative type. These results are also of importance for the fundamental studies on the optical responses of surfaces and interfaces.

Most of the experiments discussed in this Letter were performed on an on-axis (001) face (miscut <0.017°). The single-domain 2×1 surface was prepared by employing the electromigration technique as described below. A piece of Si(001) wafer was cleaned according to the standard wet-chemical method. It was then set in an ultrahigh vacuum (UHV) chamber which was evacuated by two turbo molecular pumps coupled in tandem. Both sample preparation and the RDS measurements were carried out in this chamber. The sample was heated with a dc current using Ta electrodes. To form a single-domain 2×1 surface, the sample was degassed at 920 K, flashed to 1470 K for 10 s, then annealed at 1170 K with the dc current flowing in the step-up direction [8]. The annealing was repeated until a well-ordered surface was obtained. A UHV condition in the 10^{-8} Pa range was maintained throughout the flashing and annealing processes. Formation of the single-domain surface was verified by the reflection high-energy electron diffraction method. Observation by atomic force microscopy showed that a surface prepared in this way has large terraces ($\sim 5 \ \mu$m wide) separated by double-high steps.

The RDS system used in this study adopts the photoelastic modulation method developed by Aspnes and Studna [13]. The RD signal is defined as $\Delta \tilde{r}/\tilde{r} = 2(\tilde{r}_{\bar{1}10} - \tilde{r}_{110})/(\tilde{r}_{\bar{1}10} + \tilde{r}_{110})$, where $\tilde{r}_{\bar{1}10}$ and $\tilde{r}_{110}$ are the complex field reflectance for normal-incident light with polarization along the $[\bar{1}10]$ and $[110]$ directions, respectively. We define the $[\bar{1}10]$ direction to be parallel to the dimer bonds in the dominant domain. In this Letter, only the data for the real part of the RD signal, $\Delta r/r$, are shown.

The RD spectrum for the 2×1 reconstruction on the on-axis Si(001) face is shown as spectrum (i) in Fig. 1. It agrees with the results reported by Shioda and van der Weide [12], except for the small differences in the peak amplitude and the baseline offset. The broad negative peak near 3.6 eV was previously ascribed to the transition between the backbond and empty dangling-bond states of the asymmetric dimers [11].
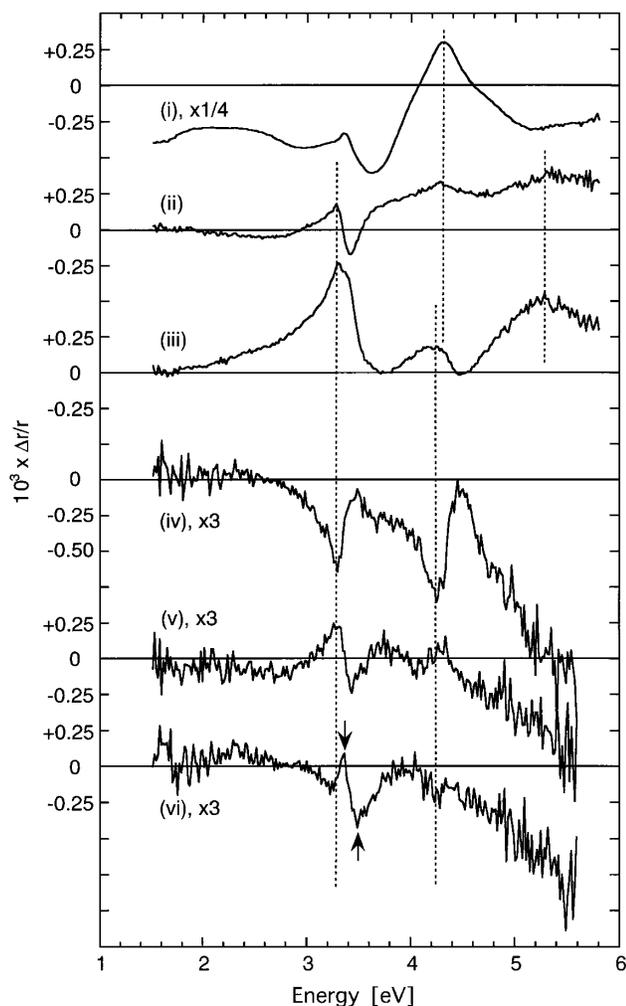
The oxidation experiments proceeded by repeating 50 times the cycle of oxidation at an elevated temperature followed by an RDS measurement at room temperature. To oxidize the sample, an O_2 gas (99.9999% purity) was supplied to a pressure of 1.3×10^{-2} Pa, and then the sample was heated at a preset temperature for a given period. Figure 2(a) shows the time-temperature diagram for the oxidation experiment. Under these conditions, oxidation of Si proceeds in the layer-by-layer mode [4]. Since the oxidation rate rapidly decreases with increasing the oxide thickness, the sample temperature was gradually increased with the oxidation time.

In Fig. 1, we show five spectra [(ii) through (vi)] selected from the fifty spectra acquired sequentially with increasing the oxidation time. The point at which each spectrum was measured is indicated in Fig. 2(a) by an arrow with the corresponding label. Upon the exposure to O_2 at room temperature [spectrum (ii)], the dimer-originated negative peak at 3.6 eV disappears, and a new feature appears near the energy of the E_1 transition in Si, with its positive and negative peaks located at 3.28 and 3.42 eV, respectively. The positive peak near 4.26 eV in spectrum (i), which is close to the E_2 transition energy, is reduced in amplitude but remains observable. Oxidation at 993 K for 8 s [spectrum (iii)] dramatically changes the
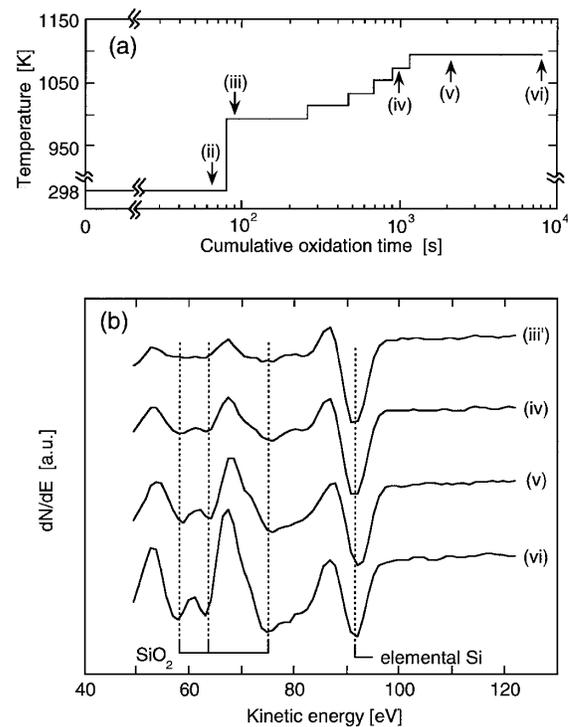
FIG. 1. Changes of the RD spectra as the single-domain Si(001)-(2×1) surface is oxidized. Spectrum (i) is for the initial Si surface. See the corresponding arrows in Fig. 2(a) for the oxidation condition for each spectrum from (ii) to (vi). Spectra (i), (iv), (v), and (vi) are expanded or reduced as noted in the plot.

FIG. 2. (a) A temperature-time diagram for the oxidation experiment in Fig. 1. The O_2 pressure was kept at 1.3×10^{-2} Pa throughout the experiment. The vertical arrows indicate the points where the AES spectra in plot (b) and RD spectra of Fig. 1 with the corresponding labels were measured. (b) Si LVV Auger features for the samples oxidized according to the diagram in (a). The main spectral features of SiO_2 and elemental Si are indicated in the plot.

spectral line shape, giving rise to a large positive peak at 3.28 eV. In addition, the peak near the E_2 energy changes its shape and a broad band evolves near 5.3 eV. The overall spectral line shape is similar to, but different in the details from, those of the energy-derivative type reported for the Si(113) surfaces, as discussed later in the text [14,15].

Continued oxidation induced further changes in the spectrum. Most importantly, *the features identified in spectrum (iii) invert their polarity,* and the spectrum evolves into the one shown as (iv) in Fig. 1. Its line shape is nearly symmetrical to that of spectrum (iii), aside from the reduced amplitude for the former. The polarity change of the RD signal is repeated as the sample is further oxidized. For example, the sign of the peaks at 3.28 and 4.26 eV changes back to positive in spectrum (v). After oxidization for 7900 s [spectrum (vi)], the peak at 3.28 eV becomes negative again, while additional features are clearly seen at the higher energies as indicated by the arrows in the plot. Thus, the progression of the oxidation induces the oscillation of the main features near the E_1 and E_2 transition energies.

The experiments were also carried out on the vicinal (001) faces miscut by 4° toward [110]. The changes of the RD spectra upon oxidation were essentially the same as those in Fig. 1, indicating that the terrace width has only minor effects on the optical anisotropy of the oxidized samples.

We argue that each inversion of the sign of the RD signal in Fig. 1 is a consequence of progression of the oxidation by one monolayer (ML). Auger electron spectroscopy (AES) was employed to estimate the oxide thickness for the sample yielding spectrum (vi) in Fig. 1, as well as for three other samples that were oxidized under the identical conditions to those for spectra (iii), (iv), and (v). Shown in Fig. 2(b) are the Si *LVV* spectra for these samples. The oxide thickness can be estimated quantitatively by taking into account the escape depth of the electrons, 0.6 nm near the Si *LVV* energy [16]. The estimated values for spectra (iii), (iv), (v), and (vi) are 0.2, 0.5, 0.7, and 1.0 nm, respectively. Validity of the thickness estimation by AES was previously cross-checked by measuring the oxide thickness using transmission electron microscopy. Since the oxidation of Si expands the volume by a factor of 2.3 [17], the oxidation by 1 ML (0.136 nm) on the (001) face should increase the oxide thickness by 0.31 nm if the expansion occurs in the surface-normal direction only. Recalling that this value is the maximum estimate, it reasonably agrees with the increment of the oxide thickness estimated as above, ~0.25 nm per 1 ML oxidation.

The significance of the above results for the oxidation studies is obvious. Namely, by monitoring the RD oscillation in real time during oxidation, it is now possible for us to *count* the number of the oxidized Si layers. Shown in Fig. 3 is the dynamic change of the RD signal at 2.90 eV as the (2×1)-reconstructed surface was oxidized. The measurement was done *in situ* during the oxidation
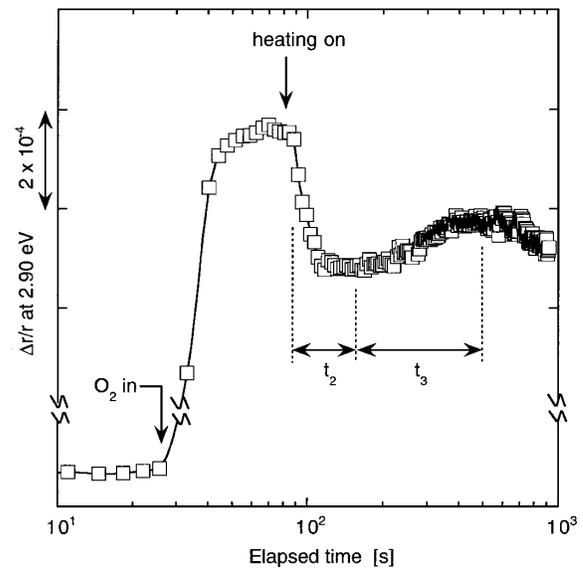

FIG. 3. The dynamic change of the RD signal at 2.90 eV as a Si(001)-(2×1) surface with a 4° miscut is oxidized under an O_2 pressure of 6×10^{-2} Pa at 1095 K. The sample temperature reached the steady state immediately (<3 s) upon turning on the heating current at 80 s.

under an O_2 pressure of 6×10^{-2} Pa at 1095 K. The initial single-domain surface for this experiment was prepared by use of a 4°-miscut wafer. The trace in Fig. 3 shows an oscillation with amplitude consistent with the spectroscopic results in Fig. 1. The half periods, t_2 and t_3, as defined in Fig. 3 represent the time required to complete the oxidation of the second and third monolayer, respectively. The oxidation of the first monolayer took place in a very short time (<1 s) under the above-mentioned condition, so its completion, which should appear as a positive peak, could not be detected in this experiment. Successful observation of the RD oscillation in Fig. 3 opens up a way for us to study the oxidation phenomenon in the layer-resolved manner.

We speculate that the fast damping of the oscillation amplitude infers that the single-domain SiO_2-Si(001) interface is energetically unfavorable, and atomic-scale roughness is introduced at the interface to lower the energy. The oscillation was best observed at the measurement energies slightly lower than 3.28 eV, because the sample heating induces the redshift of the optical transitions [18].

The spectral line shapes for the oxidized surfaces are of interest from the viewpoint of surface optics. Figure 4(a) compares spectrum (iii) to that obtained for a Si(113) surface covered with a native-oxide layer. The previous studies concluded that the major peaks in the (113) spectra are ascribed to the dichroic threshold energies and broadening parameters for the bulk critical points [14,15]. The line shapes are similar between the (001) and (113) spectra, in particular, near the E_1 transition energy. This indicates that the origin of the optical anisotropy for the (001) face is the same as for the (113) face and that the transitions
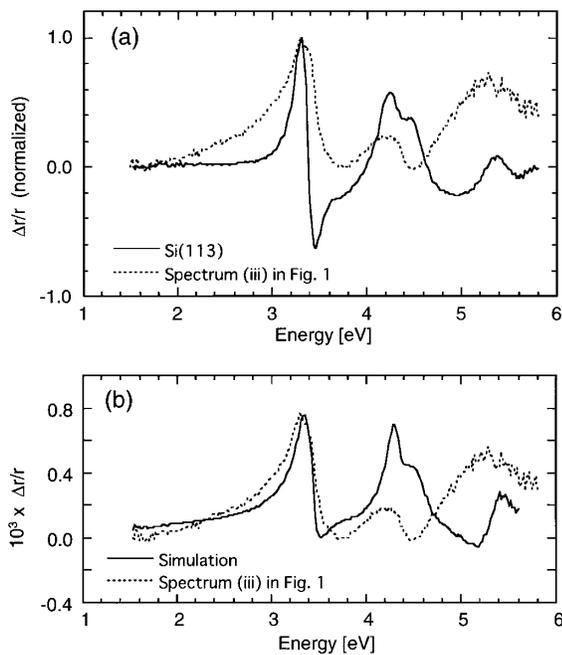
FIG. 4. (a) A comparison of the spectrum (i) in Fig. 1 to that for the Si(113) sample covered by native oxide. The spectra are normalized with respect to the peak intensity at 3.3 eV. (b) Simulation of spectrum (iii) in Fig. 1 as described in the text. Shown by the solid line is the best fit obtained for $\Delta E_g = -0.99$ meV and $\Delta\Gamma = -0.84$ meV.

involving the interface-localized states have only a minor contribution.

Mantese *et al.* reported that the (113) spectrum can be fit by using the expression which considers the anisotropy that is uniform within the penetration depth of light [7,15].

$$\frac{\Delta\tilde{r}}{\tilde{r}} = \frac{\Delta\tilde{\varepsilon}}{\tilde{n}(\tilde{n}^2 - 1)}. \tag{1}$$

Here, $\tilde{n}$ and $\Delta\tilde{\varepsilon}$ are the complex refractive index and the anisotropy in the complex dielectric function of the substrate, respectively. In their simulation, it was assumed that $\Delta\tilde{\varepsilon}$ can be expressed for each of the E_1 and E_2 transitions by a linear combination of first and second derivatives of the complex dielectric function, $d\tilde{\varepsilon}/dE$ and $d^2\tilde{\varepsilon}/dE^2$, respectively. In Fig. 4(a), the peak near the E_1 transition energy is much broader for (001) than for (113). This means that the first-derivative contribution dominates for the (001) face. In Fig. 4(b), we show the result of the simulation following the same procedures as reported by Mantese *et al.*, except for omitting the contribution of $d^2\tilde{\varepsilon}/dE^2$ [15]. Namely, $\Delta\tilde{\varepsilon}$ in Eq. (1) near the E_1 transition energy is calculated as follows:

$$\Delta\tilde{\varepsilon} = (-\Delta E_g + i\Delta\Gamma)\frac{d\tilde{\varepsilon}}{dE}. \tag{2}$$

Here, ΔE_g and $\Delta\Gamma$ are the anisotropies in the threshold energy and broadening parameter for the E_1 transition. A good fit was obtained below 4 eV with $\Delta E_g = -0.99$ meV and $\Delta\Gamma = -0.84$ meV. If we employ another optical model which assumes that the anisotropy is localized near the surface [7], the fitting is not satisfac-

tory. It is therefore concluded that the layer exhibiting the dichroic optical responses is thicker than the penetration depth of light in Si (11 nm at 3.4 eV) [15]. We failed to fit the features near and above the E_2 transition energy by any possible combination of ΔE_g and $\Delta\Gamma$.

The mechanism giving rise to the dichroism in the threshold energy and broadening parameter has been under debate since it was first reported on Si(113) [14]. While Aspnes *et al.* pointed out the importance of the dynamic localization of the photon-generated electrons and holes [19], it has also been argued that the slab calculation can reproduce the derivative line shape through modulation of the bulk states by the surface or interface [6,20]. The results reported in this Letter hopefully serve as a model case to test the theories. Here we point out only that the observed anisotropy cannot be accounted for by the strain at the SiO_2-Si interface, since the observed spectra are qualitatively different from those expected from the spectral dependence of the relevant piezo-optic tensors [21].

*Electronic address: yasuda-t@aist.go.jp
[1] E. H. Nicollian and J. R. Brews, *MOS (Metal-Oxide-Semi-conductor) Physics and Technology* (Wiley-Interscience, New York, 1982), Chap. 13.
[2] I. J. R. Baumvol, Surf. Sci. Rep. **36**, 1 (1999).
[3] F. M. Ross, J. M. Gibson, and R. D. Twesten, Surf. Sci. **310**, 243 (1994).
[4] H. Watanabe *et al.,* Phys. Rev. Lett. **80**, 345 (1998).
[5] K. Kato and T. Uda, Phys. Rev. B **62**, 15 978 (2000).
[6] T. Nakayama and M. Murayama, Appl. Phys. Lett. **77**, 4286 (2000).
[7] D. E. Aspnes and A. A. Studna, Phys. Rev. Lett. **54**, 1956 (1985).
[8] T. Doi *et al.,* Phys. Rev. B **53**, 16 609 (1996).
[9] P. E. Wierengna, J. A. Kubby, and J. E. Griffith, Phys. Rev. Lett. **59**, 2169 (1987).
[10] T. Yasuda *et al.,* Phys. Rev. Lett. **74**, 3431 (1995).
[11] L. Kipp *et al.,* Phys. Rev. Lett. **76**, 2810 (1996).
[12] R. Shioda and Y. van der Weide, Phys. Rev. B **57**, R6823 (1998).
[13] D. E. Aspnes *et al.,* J. Vac. Sci. Technol. **6**, 1327 (1988).
[14] T. Yasuda *et al.,* J. Vac. Sci. Technol. A **12**, 1152 (1994).
[15] L. Mantese *et al.,* Thin Solid Films **313–314**, 557 (1998).
[16] F. J. Himpsel *et al.,* Phys. Rev. B **38**, 6084 (1988).
[17] T. J. Delph, J. Appl. Phys. **83**, 786 (1998).
[18] J. Sik, J. Hora, and J. Humlicek, J. Appl. Phys. **84**, 6291 (1998).
[19] D. E. Aspnes, L. Mantese, and K. A. Bell, J. Vac. Sci. Technol. B **16**, 2367 (1998).
[20] R. Del Sole and G. Onida, Phys. Rev. B **60**, 5523 (1999).
[21] P. Etchegoin, J. Kircher, and M. Cardona, Phys. Rev. B **47**, 10 292 (1993).